

Possibilities of synthesis of new superheavy nuclei in actinide-based fusion reactions

G. G. Adamian,^{1,2} N. V. Antonenko,¹ and W. Scheid³

¹Joint Institute for Nuclear Research, 141980 Dubna, Russia

²Institute of Nuclear Physics, 702132 Tashkent, Uzbekistan

³Institut für Theoretische Physik der Justus-Liebig-Universität, D-35392 Giessen, Germany

(Received 3 December 2003; published 1 April 2004)

The actinide-based hot fusion reactions with stable projectiles heavier than ^{48}Ca are analyzed within the dinuclear system model for compound nucleus formation. The production of the odd superheavy nuclei in the ^{48}Ca -induced hot fusion reactions is considered. Predictions for several reactions with radioactive beams of ^{46}Ar , ^{47}K , and ^{50}Ca for the synthesis of heaviest elements are also presented for the future interest.

DOI: 10.1103/PhysRevC.69.044601

PACS number(s): 25.70.Jj, 24.10.-i, 24.60.-k, 27.90.+b

The ^{48}Ca -induced hot fusion reactions with some actinide targets were carried out in Dubna [1] in order to approach to “the island of stability” of superheavy elements (SHE) predicted at charge numbers $Z=114-126$ and neutron numbers $N=172-184$ by the nuclear shell models [2,3]. The further experimental extension of the region of SHE is limited by the number of available projectiles and targets, and by very low production cross section [1,3]. Since the intensive radioactive ion beams are not available so far, the possible way to synthesize new SHE is to use the actinide-based reactions with projectiles heavier than ^{48}Ca . However, as in case of cold ^{208}Pb - and ^{209}Bi -based fusion reactions one can expect the strong decrease of the evaporation residue cross section with increasing charge number of projectile due to the increase of repulsive Coulomb forces. In the present paper we analyze the actinide-based reactions with different stable and radioactive projectiles and recommend for the experimental study those which lead to the evaporation residue cross sections above the present experimental limit of registration (about 0.1 pb). With ^{48}Ca beam the production of superheavies with odd Z is investigated as well.

The fusion is described by the dinuclear system (DNS) model [4–7] in which the evaporation residue cross section is factorized as follows:

$$\sigma_{ER}(E_{c.m.}) = \sigma_c(E_{c.m.})P_{CN}(E_{c.m.})W_{sur}(E_{c.m.}). \quad (1)$$

Here, $\sigma_c = \pi\chi^2(J_{max}+1)^2T(E_{c.m.})$ is the effective capture cross section for the transition of the colliding nuclei over the entrance (Coulomb) barrier with the transmission probability T [5], P_{CN} is the fusion probability, and W_{sur} is the survival probability of excited compound nucleus in the deexcitation process. The contributing angular momenta in the evaporation residue cross section are limited by W_{sur} with $J_{max} \approx 10$ when highly fissile excited superheavy nuclei are produced for energies $E_{c.m.}$ above the Coulomb barrier [5,6].

In the DNS fusion model the compound nucleus is reached by a series of transfers of nucleons from the light nucleus to the heavy one [4–7]. The DNS has two main degrees of freedom: the mass asymmetry $\eta=(A_1-A_2)/(A_1+A_2)$ (A_1 and A_2 are the mass numbers of the DNS nuclei) and the relative distance R between the centers of the DNS

nuclei. The dynamics of the DNS is considered as a combined diffusion in coordinates η and R . The diffusion in R occurs towards the values larger than the sum of the radii of the DNS nuclei and finally leads to the quasifission (decay of the DNS in R). The basic assumption of the DNS model that the touching nuclei are hindered by a repulsive potential to amalgamate directly in R into compound nucleus. The fusion probability P_{CN} gives the probability that the DNS crosses the inner fusion barrier B_{fus}^* in η and forms the compound nucleus. P_{CN} can be calculated by solving diffusion equations like the Fokker-Planck and master equations in coordinates η and R or by using the Kramers approximation [8,9]. The probability of complete fusion is calculated in the following way:

$$P_{CN} = \lambda_{\eta}^{Kr} / (\lambda_{\eta}^{Kr} + \lambda_{\eta_{sym}}^{Kr} + \lambda_R^{Kr}). \quad (2)$$

Since the initial DNS is in the conditional minimum of potential energy surface, we use a two-dimensional Kramers-type expression for the quasistationary rates λ_{η}^{Kr} of the fusion, $\lambda_{\eta_{sym}}^{Kr}$ of the symmetrization of the DNS with the following decay and λ_R^{Kr} of the quasifission from the initial DNS through the fusion barrier B_{fus}^* in η , through the barrier $B_{\eta_{sym}}$ in η in the direction to more symmetric DNS configurations and through the quasifission barrier B_{qf} in R , respectively [6,7]. The main factor which prohibits the complete fusion of heavy nuclei is the evolution of the initial DNS to more symmetric configurations [$B_{\eta_{sym}} \approx (0.5-1.5)$ MeV and $(4-5)$ MeV for hot and cold fusion, respectively] and decay of the DNS during this process or the decay of the initial DNS. In hot fusion reactions, the decay of DNS takes place mainly outside of the initial conditional minimum because $B_{qf} > B_{\eta_{sym}}$ in contrast to the case of cold fusion reactions. The local temperature Θ of the initial DNS calculated with the Fermi-gas model expression $\Theta = \sqrt{E^*}/a$ ($a = A_{CN}/12$ MeV $^{-1}$, $A_{CN} = A_1 + A_2$, and E^* is the excitation energy of the DNS) is used in λ_{η}^{Kr} , $\lambda_{\eta_{sym}}^{Kr}$, and λ_R^{Kr} [6].

The barriers B_{fus}^* , $B_{\eta_{sym}}$, and B_{qf} are given by the potential energy of the DNS which is calculated as the sum of binding energies B_i of the nuclei ($i=1, 2$) and of the nucleus-nucleus potential V [4–6]: $U(R, \eta) = B_1 + B_2 + V(R, \eta)$. V is calculated

with the double-folding procedure with a nuclear radius parameter $r_0 = 1.15$ fm and a diffuseness $a_0 = 0.54 - 0.56$ fm depending on the mass number of the isotope. The variations of the potential in η are caused by both shell effects and odd-even effects included into the calculations through realistic binding energies [10–13]. The isotopic composition of the nuclei forming the DNS is obtained with the condition of a N/Z equilibrium in the system. The potential of the DNS depends on the ground state deformations [14] of the nuclei assumed in the pole-pole orientation.

The survival probability under the evaporation of x neutrons is treated according to Refs. [6,7,15,16] as

$$W_{sur} = P_{xn}(E_{CN}^*) \prod_{i=1}^x \frac{\Gamma_n[(E_{CN}^*)_i]}{\Gamma_n[(E_{CN}^*)_i] + \Gamma_f[(E_{CN}^*)_i]},$$

$$\frac{\Gamma_n}{\Gamma_f} = \frac{0.41A^{2/3}a_f U_n}{2[a_n U_n]^{1/2} - 1} \exp[2a_n^{1/2} U_n^{1/2} - 2a_f^{1/2} U_f^{1/2}],$$

where P_{xn} is the probability for the realization of the xn channel at the excitation energy $E_{CN}^* = E_{c.m.} + Q$ of the compound nucleus and i is the index of the evaporation step [16]. $(E_{CN}^*)_i$ is the mean value of excitation energy of the compound nucleus at the beginning of step i with $(E_{CN}^*)_1 = E_{CN}^*$. We used the analytical expression for the ratio of the partial widths of neutron emission (Γ_n) and fission (Γ_f) in Eq. (3), and $U_n = E_{CN}^* - B_n - \delta$, $U_f = E_{CN}^* - (B_f - \delta) \exp[-E_{CN}^*/E_d] - \delta$ [9,17]. The neutron binding energies B_n and the absolute values of microscopic corrections as fission barriers $B_f(E_{CN}^* = 0)$ are taken from different mass tables [11–13]. In Fermi-gas approximation B_f value depends on E_{CN}^* as $B_f = B_f(E_{CN}^* = 0) \exp[-E_{CN}^*/E_d]$ where $E_d = 25$ MeV is the shell-damping energy [15]. At the excitation energies of (30–50) MeV in hot fusion reactions the damping of the shell corrections reduces the difference between the results obtained with various predictions of the properties of superheavies. The pairing corrections $\delta = 22/A_0^{1/2}$ and $11/A_0^{1/2}$ for even-even and odd-even nuclei (odd-even effect), respectively, were taken into consideration. In U_f a double counting of pairing in the fission barrier, which is a purely shell correction, was avoided. The ratio of the level density parameters in the fission and neutron evaporation channels is chosen as $a_f/a_n = 1.07$ and $1.045(a_n = a)$ for the predictions of Ref. [11] and Refs. [12,13], respectively, in order to describe the experimental evaporation residue cross section for the reaction $^{48}\text{Ca} + ^{244}\text{Pu} \rightarrow ^{288}114 + 4n$ [7]. The predictions of Refs. [12,13] give the same fission barrier but different values of B_n . Since the value of a_f/a_n is related to the rate of the change of nuclear structure from the ground state to the saddle point [17], smaller $B_f(E_{CN}^* = 0)$ in Refs. [12,13] than in Ref. [11] requires slightly smaller a_f/a_n .

It is very difficult to estimate σ_{ER} by looking only at the predicted value of fission barrier of compound nucleus. Besides the values of fission barriers, the neutron separation energies, and Q values are important for the calculation of W_{sur} and σ_{ER} in the region of superheavies. The fusion probability P_{CN} depends also on the predicted mass of nuclei with $Z > 102$ because the DNS potential energy is a function of

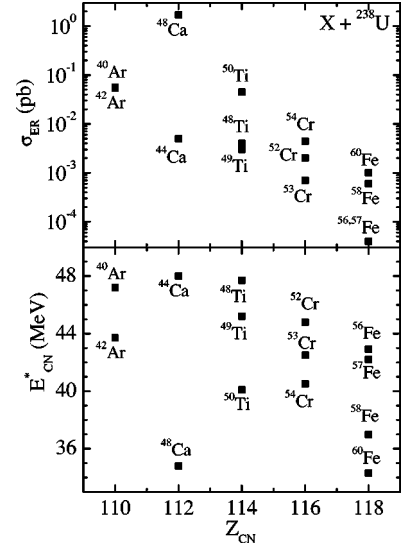


FIG. 1. The calculated maximal evaporation residue cross sections (upper part) at the corresponding optimal excitation energies of the compound nuclei for the ^{238}U -based hot fusion reactions. The predictions of Ref. [11] were used in the calculations.

mass asymmetry coordinate. For the calculation of σ_{ER} , we presently have no complete set of predicted properties of superheavies in the framework of the relativistic mean-field models. The nonrelativistic mean-field model [18] gives the complete set but results unusually large pairing strength (about 3 MeV). The predictions of macroscopic-microscopic models [11–13] provide us all values which are necessary for the calculations of σ_{ER} and have good theoretical background.

The previous DNS model calculations of σ_{ER} and optimal bombarding energy for cold and hot fusion reactions leading to heavy and superheavy nuclei, and of mass (charge) and kinetic energy distributions of the products of quasifission, which accompanies the fusion process, were in good agreement with available experimental data [4–7,19]. This allows us to be confident in our predictions. The estimated inaccuracy of our calculations of σ_{ER} is within factor of 2–4. The inaccuracy in the definition of B_{fus}^* creates an inaccuracy within a factor of 2 in the calculation of σ_{ER} . Since the calculations for all reactions were performed with the same parameters and assumptions, the prediction of the relative values of cross sections is quite high.

The calculated evaporation residue cross sections σ_{ER} at the maxima of excitation functions and the corresponding excitation energies E_{CN}^* of the compound nuclei are plotted in Figs. 1–3 for various ^{238}U -based reactions. In Figs. 1–3 σ_{ER} and E_{CN}^* are estimated using the predictions of the properties of superheavies from Refs. [11–13], respectively. The extraordinary low excitation energy in the $^{48}\text{Ca} + ^{238}\text{U}$ reaction is due to the gain in the Q value. With projectiles heavier than ^{48}Ca E_{CN}^* becomes smaller with increasing mass A_{CN} numbers of compound nucleus. The predicted cross sections are almost independent within the factor of 2–5 on the choice of the mass table. This variation is almost within the inaccuracy of calculation. The advantage of ^{48}Ca beam is evident. The calculated evaporation residue cross sections decreases

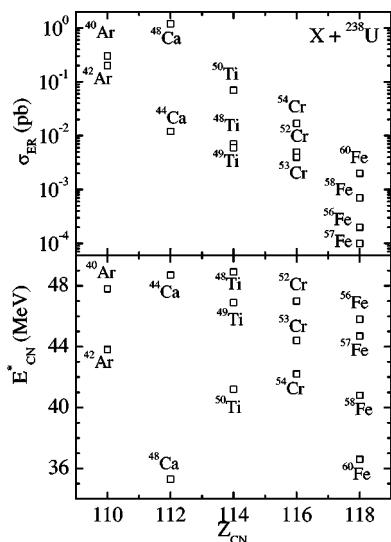


FIG. 2. The same as in Fig. 1, but with the predictions of Ref. [12].

by about 3 orders of magnitude with increasing the charge number of projectile from 20 to 26. The main reason of fall-off of σ_{ER} is the strong decrease of fusion probability P_{CN} . The quasifission in the DNS becomes much stronger than the complete fusion with increasing charge number of compound nucleus. Besides ^{48}Ca , only the projectiles $^{40,42}\text{Ar}$ and ^{50}Ti result the cross section on the level of the present experimental possibilities. The same dependence of σ_{ER} on the projectile one can observe with other actinide targets. For instance, for the reactions $^{50}\text{Ti} + ^{241}\text{Pu}$, $^{54}\text{Cr} + ^{241}\text{Pu}$, and $^{58}\text{Fe} + ^{241}\text{Pu}$ we obtained $\sigma_{ER} = 2 \times 10^{-2}$ pb, 2×10^{-3} pb, and 3×10^{-6} pb at $E_{CN}^* = 36.7$ MeV, 35.7 MeV, and 34.5 MeV, respectively. The reactions with ^{241}Pu target are more favorable than the reactions with $^{242,244}\text{Pu}$ targets [7]. Another example is the reactions with thorium target: for $^{50}\text{Ti} + ^{232}\text{Th}$, $^{54}\text{Cr} + ^{232}\text{Th}$, $^{58}\text{Fe} + ^{232}\text{Th}$, and $^{64}\text{Ni} + ^{232}\text{Th}$, we ob-

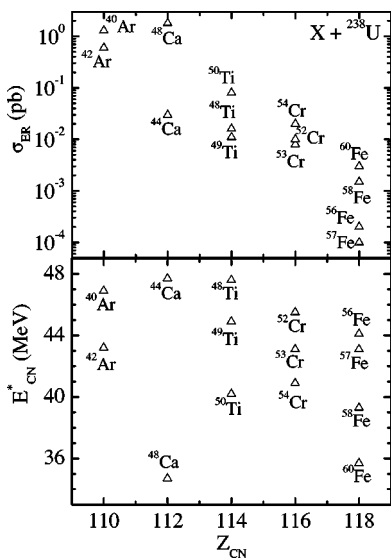


FIG. 3. The same as in Fig. 1, but with the predictions of Ref. [13].

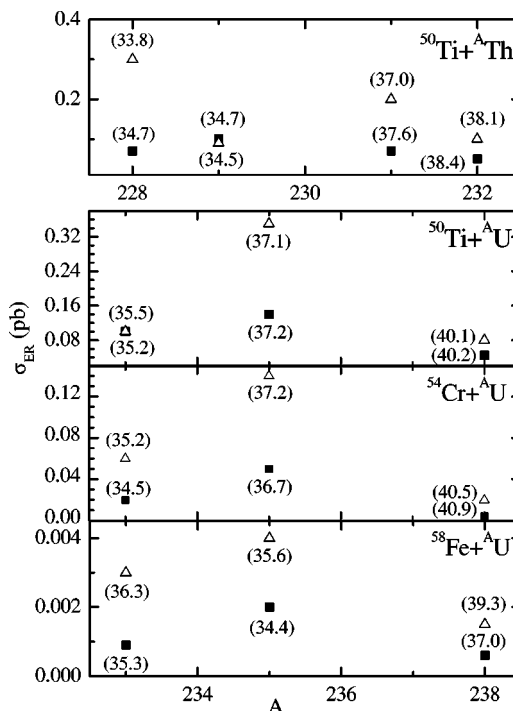


FIG. 4. The calculated maximal evaporation residue cross sections at the corresponding optimal excitation energies of the compound nuclei (in parenthesis) for the hot fusion reactions as a function of mass number A of the target. The results obtained with the predictions of Refs. [11] and [13] are shown by closed squares and open triangles, respectively.

tained $\sigma_{ER} = 5 \times 10^{-2}$ pb, 10^{-1} pb, 10^{-2} pb, and 8×10^{-4} pb at $E_{CN}^* = 38.4$ MeV, 38.5 MeV, 38.4 MeV, and 31 MeV, respectively. All calculations above are performed using the mass table of Ref. [11].

From Figs. 1–3 one can conclude that the stable isotopes of projectile nucleus with the largest neutron excess are favorable for the most cases of hot fusion. At fixed charge asymmetry in the entrance channel, the fusion probability P_{CN} and excitation energy E_{CN}^* of compound nucleus decrease with increasing neutron excess in the projectile. The gain in the survival probability W_{sur} is not compensated by the loss in P_{CN} .

From Figs. 4–6 one can see that the reactions with smaller neutron excess in the target within certain interval of A are even more favorable for producing of SHE than those with larger neutron excess. The value of P_{CN} becomes larger with decreasing A in most cases. In these reactions the Q value and, thus, E_{CN}^* decrease with A in the considered intervals. This behavior was also observed within a certain small interval of A in the case of ^{48}Ca -induced Ra-, Th-, U-, Pu-, Cm-, and Cf-based fusion reactions [7].

From our calculations shown in Figs. 5 and 6 one can expect quite large cross sections in the actinide-based reactions with a ^{48}Ca beam and targets ^{236}Np , ^{242}Am , and ^{248}Bk for the production of odd SHE with charge numbers 113, 115, and 117, respectively. For the reactions $^{48}\text{Ca} + ^{227}\text{As}$, ^{231}Pa and $^{252,254}\text{Es}$ leading to 109, 111, and 119 elements, we obtained $\sigma_{ER} = 7.9/10.2/25.7$ pb, $1.0/2.2/4.4$ pb, $0.006/0.018/0.013$ pb, and $0.01/0.015/0.02$ pb at $E_{CN}^* =$

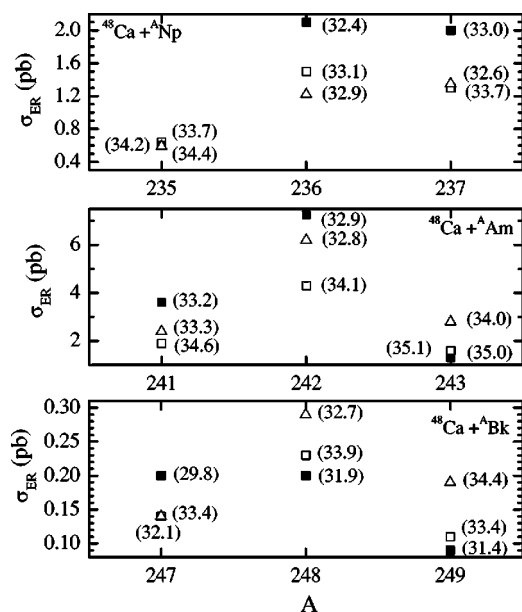


FIG. 5. The calculated maximal evaporation residue cross sections at the corresponding optimal excitation energies of the compound nuclei (in parenthesis) for the hot fusion reactions $^{48}\text{Ca} + ^A\text{Np}$, $^{48}\text{Ca} + ^A\text{Am}$, $^{48}\text{Ca} + ^A\text{Bk}$ as a function of A . The results obtained with the predictions of Ref. [11], Ref. [12], and Ref. [13] are shown by closed squares, open squares, and open triangles, respectively.

32.3/33.3/32.5 MeV, 31.7/32.4/31.3 MeV, 29.8/30.8/30.4 MeV, and 28.2/31.0/29.9 MeV, respectively, using the mass tables from Ref. [11]/Ref. [12]/Ref. [13].

The radioactive beams of ^{47}K and ^{46}Ar are likely produced with high intensities in near future. In the actinide-based reactions the use of neutron-rich projectiles of ^{47}K and ^{50}Ca leads to the values of σ_{ER} comparable with one for the reactions with ^{48}Ca (Fig. 6). However, with these projectiles one can produce new odd SHE with the neutron number closed to $N=184$. For the reaction $^{46}\text{Ar} + ^{248}\text{Cm}$, we obtained $\sigma_{ER}=9$ pb at $E_{CN}^*=38$ MeV using the predictions of Ref. [11].

Our conclusions are the following. (1) In the actinide-based reactions the gain in survival probability with increasing neutron excess in the stable projectile is not compensated by the loss in complete fusion probability. (2) In ^{48}Ca -induced hot fusion reactions the stable actinide targets with smaller neutron excess (within certain intervals of mass)

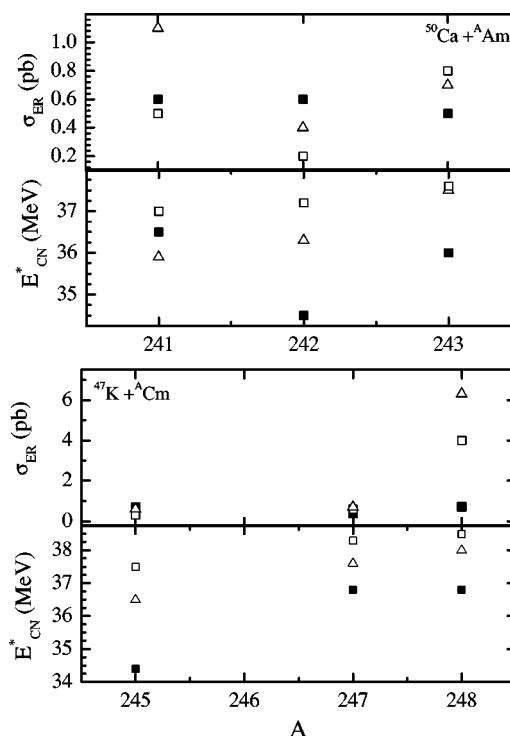


FIG. 6. The same as in Fig. 5, but for the hot fusion reactions $^{50}\text{Ca} + ^A\text{Am}$ and $^{47}\text{K} + ^A\text{Cm}$.

are even more favorable than those with larger neutron excess. The reactions $^{48}\text{Ca} + ^{236}\text{Np}$, ^{242}Am , ^{248}Bk are most favorable for the production of odd SHE with charge numbers 113, 115, and 117. (3) For the first time, we show that the actinide-based reactions with stable projectiles heavier than ^{50}Ti projectile are not much promising for further synthesis of SHE. (4) The radioactive projectiles are not much favorable in comparison to the stable projectiles. (5) New isotopes of SHE with $Z=110$, 112, 114, and 115 could be produced in the reactions $^{40,42}\text{Ar} + ^{238}\text{U}$, $^{50}\text{Ti} + ^{228,229,231}\text{Th}$, ^{235}U , and ^{46}Ar , $^{47}\text{K} + ^{248}\text{Cm}$. Our results could motivate the experimental efforts for producing new SHE.

We thank Professor Yu. Ts. Oganessian and Professor V. V. Volkov for fruitful discussions and suggestions. This work was supported in part by VW-Stiftung, DFG, RFBR, and STCU(Uzb-45). The Polish-JINR (Dubna) and IN2P3 (France)-JINR (Dubna) Cooperation Program are gratefully acknowledged.

- [1] Yu. Ts. Oganessian *et al.*, *Eur. Phys. J. A* **13**, 135 (2002); **15**, 201 (2002).
 [2] A. Sobiczewski, F. A. Gareev, and B. N. Kalinkin, *Phys. Lett. B* **22**, 500 (1966); P. Möller and J. R. Nix, *J. Phys. G* **20**, 1681 (1994).
 [3] S. Hofmann and G. Münzenberg, *Rev. Mod. Phys.* **72**, 733 (2000).
 [4] V. V. Volkov, *Izv. Akad. Nauk SSSR, Ser. Fiz.* **50** 1879 (1986); N. V. Antonenko *et al.*, *Phys. Lett. B* **319**, 425 (1993); *Phys.*

Rev. C **51**, 2635 (1995).

- [5] G. G. Adamian, N. V. Antonenko, and W. Scheid, *Nucl. Phys.* **A618**, 176 (1997); G. G. Adamian, N. V. Antonenko, W. Scheid, and V. V. Volkov, *ibid.* **A627**, 361 (1997); **A633**, 409 (1998); R. V. Jolos, A. K. Nasirov, and A. I. Muminov, *Eur. Phys. J. A* **4**, 245 (1999); E. A. Cherepanov, JINR Report No E7-99-27, 1999.
 [6] G. G. Adamian, N. V. Antonenko, and W. Scheid, *Nucl. Phys.* **A678**, 24 (2000).

- [7] G. G. Adamian, N. V. Antonenko, and W. Scheid, Phys. Rev. C **69**, 014607 (2004).
- [8] P. Fröbrich and R. Lipperheide, *Theory of Nuclear Reactions*, (Clarendon, Oxford, 1996).
- [9] W. U. Schröder and J. R. Huizenga, in *Treatise on Heavy-Ion Science*, edited by D. A. Bromley (Plenum, New York, 1984), Vol. 2, p. 180.
- [10] G. Audi and A. H. Wapstra, Nucl. Phys. **A565**, 1 (1993).
- [11] P. Möller and J. R. Nix, At. Data Nucl. Data Tables **39**, 213 (1988); LANL LA-UR-86-3983, 1986.
- [12] P. Möller, J. R. Nix, W. D. Myers, and W. J. Swiatecki, At. Data Nucl. Data Tables **59**, 185 (1995).
- [13] W. D. Myers and W. J. Swiatecki, Nucl. Phys. **A601**, 141 (1996); Report LBL-36803 (1994).
- [14] S. Raman, C. W. Nestor, and P. Tikkanen, At. Data Nucl. Data Tables **78**, 1 (2001).
- [15] G. G. Adamian, N. V. Antonenko, S. P. Ivanova, and W. Scheid, Phys. Rev. C **62**, 064303 (2000); A. S. Zubov *et al.*, *ibid.* **65**, 024308 (2002).
- [16] E. A. Cherepanov and A. S. Iljinov, Nukleonika **25**, 611 (1980).
- [17] R. Vandenbosch and J. R. Huizenga, *Nuclear Fission* (Academic, New York, 1973).
- [18] Y. Aboussir *et al.*, At. Data Nucl. Data Tables **61**, 127 (1995).
- [19] G. G. Adamian, N. V. Antonenko, and W. Scheid, Phys. Rev. C **68**, 034601 (2003).